The Journal of Chemical Physics ARTICLE scitation.org/journal/jcp

Toward photoswitchable electronic pre-resonance stimulated Raman probes

Cite as: J. Chem. Phys. 154, 135102 (2021); doi: 10.1063/5.0043791
Submitted: 11 January 2021 • Accepted: 15 March 2021 •
Published Online: 2 April 2021

Dongkwan Lee,[1] Chenxi Qian,[1] Haomin Wang,[1] Lei Li,[2] Kun Miao,[1] Jiajun Du,[1] Daria M. Shcherbakova,[3] Vladislav V. Verkhusha,[3,4] Lihong V. Wang,[2] and Lu Wei[1,a)]

AFFILIATIONS

[1]Division of Chemistry and Chemical Engineering, California Institute of Technology, Pasadena, California 91125, USA
[2]Division of Engineering and Applied Science, California Institute of Technology, Pasadena, California 91125, USA
[3]Department of Anatomy and Structural Biology, and Gruss-Lipper Biophotonics Center, Albert Einstein College of Medicine, Bronx, New York 10461, USA
[4]Medicum, Faculty of Medicine, University of Helsinki, Helsinki, Finland

Note: This paper is part of the 2021 JCP Emerging Investigators Special Collection.
[a)]**Author to whom correspondence should be addressed:** lwei@caltech.edu

ABSTRACT

Reversibly photoswitchable probes allow for a wide variety of optical imaging applications. In particular, photoswitchable fluorescent probes have significantly facilitated the development of super-resolution microscopy. Recently, stimulated Raman scattering (SRS) imaging, a sensitive and chemical-specific optical microscopy, has proven to be a powerful live-cell imaging strategy. Driven by the advances of newly developed Raman probes, in particular the pre-resonance enhanced narrow-band vibrational probes, electronic pre-resonance SRS (epr-SRS) has achieved super-multiplex imaging with sensitivity down to 250 nM and multiplexity up to 24 colors. However, despite the high demand, photoswitchable Raman probes have yet to be developed. Here, we propose a general strategy for devising photoswitchable epr-SRS probes. Toward this goal, we exploit the molecular electronic and vibrational coupling, in which we switch the electronic states of the molecules to four different states to turn their ground-state epr-SRS signals on and off. First, we showed that inducing transitions to both the electronic excited state and triplet state can effectively diminish the SRS peaks. Second, we revealed that the epr-SRS signals can be effectively switched off in red-absorbing organic molecules through light-facilitated transitions to a reduced state. Third, we identified that photoswitchable proteins with near-infrared photoswitchable absorbance, whose states are modulable with their electronic resonances detunable toward and away from the pump photon energy, can function as the photoswitchable epr-SRS probes with desirable sensitivity (<1 μM) and low photofatigue (>40 cycles). These photophysical characterizations and proof-of-concept demonstrations should advance the development of novel photoswitchable Raman probes and open up the unexplored Raman imaging capabilities.

I. INTRODUCTION

Photoswitchable probes are molecules whose signals can be turned on and off reversibly upon irradiation of light. The development of such optical-highlighter probes could greatly expand the range of questions that can be investigated, particularly in biology. For example, the emergence of photoswitchable fluorophores has allowed unique imaging of protein dynamics in cells, sensing of subcellular environment, and optical data writing and storage.[1–5] By precisely activating and deactivating fluorescence in space and time, these probes have also largely facilitated the development of the ground-breaking super-resolution microscopy, pushing the spatial resolution of optical imaging to tens of nanometers.[6–8] Prominently, utilizing the non-fluorescent states (i.e., the OFF state) of photoswitchable fluorescent proteins, which have a much longer lifetime (> ms) compared to the fluorescence lifetime (~ ns) of excited states, RESOLFT (reversible saturable optical fluorescence transitions) has addressed the high-power photo-damage issues in

STED (stimulated emission depletion) microscopy and allows an eight-order-of-magnitude smaller illumination intensity than STED for super-resolution live-cell imaging.[9–13]

In addition to fluorescence microscopy, Raman imaging, which targets the vibrational transitions of chemical bonds, has shown its promises to be a powerful biomedical imaging modality that offers complementary information when interrogating biological systems. In particular, stimulated Raman scattering (SRS) microscopy, which harnesses the stimulated emission amplification principle, could accelerate the vibrational transitions by 10^8 times compared to spontaneous Raman [Fig. 1(a)]. Overcoming the low sensitivity issue in conventional spontaneous Raman imaging, SRS has achieved subcellular imaging with speed up to the video rate.[14,15] It allows detection of endogenous biomolecules in a label-free fashion and also offers bioorthogonal chemical imaging of small metabolites and drugs in live cells, tissues, and animals with tiny Raman tags.[16–18] However, no photoswitchable Raman probes have been reported so far.

Recently, by bringing the pump photon energy close to, but still slightly detuned away from, the electronic absorption maximum of the red-absorbing dyes, electronic pre-resonance SRS (epr-SRS) has been invented, enhancing the sensitivity of Raman imaging down to 250 nM. Such a sensitivity level is close to that offered by typical confocal fluorescence microscopy.[19,20] Compared to conventional non-resonance SRS [Fig. 1(a)], epr-SRS obtains an up to 10^5-fold signal boost while keeping the electronic-resonance-related background to a minimum level [Fig. 1(b)]. With a newly developed and synthesized probe palette, epr-SRS has enabled optical super-multiplex imaging for up to simultaneous 24-color visualization of biological targets.[19] These probes, which incorporate narrow-band and isotope edited nitrile (~11 cm^{-1}) or alkyne (~14 cm^{-1}) moieties to their conjugation systems, share similar electronic absorption peaks, but show distinctly separated Raman bands in the desired cell-silent Raman spectral region (1700–2700 cm^{-1}).[19–21]

Herein, we explore and develop the photoswitchable epr-SRS probes. Since epr-SRS probes manifest strong coupling between electronic and vibrational transitions, we use light-induced transitions from one electronic state to another as a general strategy to switch epr-SRS signals on and off. Specifically, we adopt an additional excitation beam to induce electronic state transitions of the molecules [Fig. 1(c), green arrow]. As the excitation beam depletes the ON state population to the OFF state, the SRS laser pair [Fig. 1(d), the Stokes beam fixed at 1031.2 nm and the pump beam tunable around 830–880 nm for epr-SRS imaging] is utilized to probe the depleted ON state epr-SRS vibrational modes. In principle, the epr-SRS signals could possibly be switched off and on with and without the excitation from the additional laser, respectively [Figs. 1(c) and 1(d)]. One envisioned application with such photoswitchable molecules is super-multiplex (i.e., >10 plex) super-resolution imaging, which has remained as a highly challenging but long sought-after goal.[22] Since epr-SRS probes all share similar absorption peaks, only a single doughnut depletion laser would be required to switch off the periphery signals and leave the spectrally-separated epr-SRS signals in the center (Fig. S1). As a comparison, if STED or RESOLFT were to achieve this goal of super-multiplex super-resolution, an additional pair of excitation and depletion beams is required for each extra color.[9–13] This is highly challenging due to two main reasons. First, the added laser lines and optics would largely increase the complexity for precise instrumentation alignment. Second, the existing color-barrier in fluorescence (i.e., the spectral overlap) would typically limit the number of possible colors to 3–5.[23–25]

Guided by the rationales above, we study the photophysics of different molecular electronic states to evaluate whether they can serve as an OFF state for the ground-state epr-SRS excitations. We first investigated the excited state and the triplet state to implement the ground-state depletion photoswitching strategy. We found that transitions to the first excited state and triplet state result in vanishing epr-SRS peaks but also induce large electronic background. Guided by the Albrecht A-term pre-resonance approximation equation (see the supplementary material, Scheme 1), we then revealed that a thiol-promoted long-lived dark state of organic dyes and an absorption-detuned transition state of near-infrared (NIR) proteins could effectively eliminate the epr-SRS signals and serve as the OFF states for cyclic photoswitching. We envision this work to motivate further research in developing and optimizing the

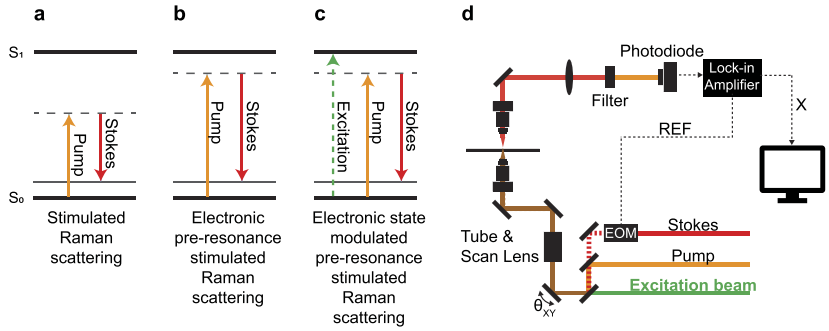

FIG. 1. Principle and design of photoswitchable electronic pre-resonance SRS (epr-SRS) via electronic state transition. [(a)–(c)] Energy diagrams of SRS (a), epr-SRS (b), and the proposed electronic-state modulated epr-SRS with an additional electronic excitation laser (green) (c). (d) Experimental scheme of the electronic-state modulated epr-SRS by introducing a third excitation beam (green) to a conventional SRS microscope. EOM, electro-optic modulator; REF, reference; and X, in-phase X-output of the lock-in amplifier.

photoswitchable epr-SRS probes and to expand the capabilities of optical imaging.

II. RESULTS

A. Photoswitching by ground-state-depletion epr-SRS

First, we explored the possibility of harnessing electronic excited states as the OFF state for epr-SRS signals [Fig. 2(a)]. It is known that bond properties (e.g., force constants, bond orders) change between the ground and excited states.[26] Recent studies have also shown that Raman spectra of molecules in the excited state exhibit shifted peaks compared to those of the ground state for certain vibrational modes in the molecules.[27,28] We hence reasoned that shifting the population to the excited state could likely deplete the ground-state Raman signals. To test this for epr-SRS, we adopted Rhodamine 800 (Rh800), a near-infrared-absorbing dye peaked around 680 nm with high and well-characterized epr-SRS signals [the structure shown in Figs. 2(b) and 2(c)].[19–21] For electronic excitation, we integrated and aligned a 660 nm continuous wave (CW) laser into the SRS system for steady state excitation [Fig. 1(d)]. We planned to excite Rh800 by the 660 nm excitation beam and simultaneously probe the ground-state epr-SRS signals by the SRS beams [Fig. 2(a), OFF state, dashed laser lines for pump and Stokes]. We would then compare the resulting epr-SRS spectra with and without 660 nm excitation for signal suppression analysis. To ensure over 80% excitation of the population from the ground state to the excited state, we applied up to 34 mW of the 660 nm excitation beam (Table S1).

Since excited-state Raman peaks are possibly shifted from those of the ground state, we expected to observe a decrease in epr-SRS signals for electronic pre-resonance enhanced peaks from Rh800 upon 660 nm excitation. We, indeed, observed a gradual decrease in the epr-SRS peaks for both the double bond [Fig. 2(b) and Fig. S2(a)] and triple bond [Fig. 2(c) and Fig. S2(b)] of Rh800 with increasing excitation beam powers. However, we simultaneously detected a large increase in the broad background [Figs. 2(b) and 2(c)]. The increase in background shows strong resemblance to the SRS spectra in the rigorous resonance regime.[19,20,29] We, hence, reasoned that the observed background increase should originate from the reduced energy gap between the first electronic excited state (S_1) and the second electronic excited state (S_2) compared to that between the ground state (S_0) and the first electronic excited state (S_1) [Fig. 2(a), OFF state]. epr-SRS excitations for the excited-state Rh800 would, therefore, invoke high rigorous-electronic-resonance-involved background [Fig. 2(a), OFF state, solid laser lines for pump and Stokes]. In addition to the peak shift that can induce peak decrease at the original epr-SRS frequency channel as we initially hypothesized, there are a few additional possible factors that may likely underlie the decrease in the epr-SRS signals upon 660 nm excitation even without a peak shift. One possibility is the population competition between the epr-SRS excitation and the invoked rigorous-electronic-resonance-involved four-wave mixing processes.[19] Second, since the frequency-independent K term in the Albrecht A equation includes a quadratic dependence on the oscillation strength of the molecular absorption (i.e., σ_{abs}), a smaller σ_{abs} for the S_1–S_2 transition compared to that of the S_0–S_1 transition may also lead to a much-lowered excited-state epr-SRS peaks.

The invoked high electronic background from the excited state would complicate the analysis for imaging applications. In principle, utilizing a frequency-modulation SRS scheme, which subtracts SRS signals between on-resonance and off-resonance frequencies in real-time[30,31] instead of the intensity-modulation SRS scheme in our setup, should resolve this issue. Nonetheless, it is still desirable to have a high signal-to-background ratio for straightforward imaging interpretations. Since the background is potentially induced by the S_1–S_2 transition, we then aimed at investigating whether the triplet state (T_1) could serve as an OFF state for epr-SRS signals with a decreased background [Fig. 3(a)]. To increase the T_1 population, we added potassium iodide (KI) to the dye solution, which is known to accelerate intersystem crossing by the heavy atom induced

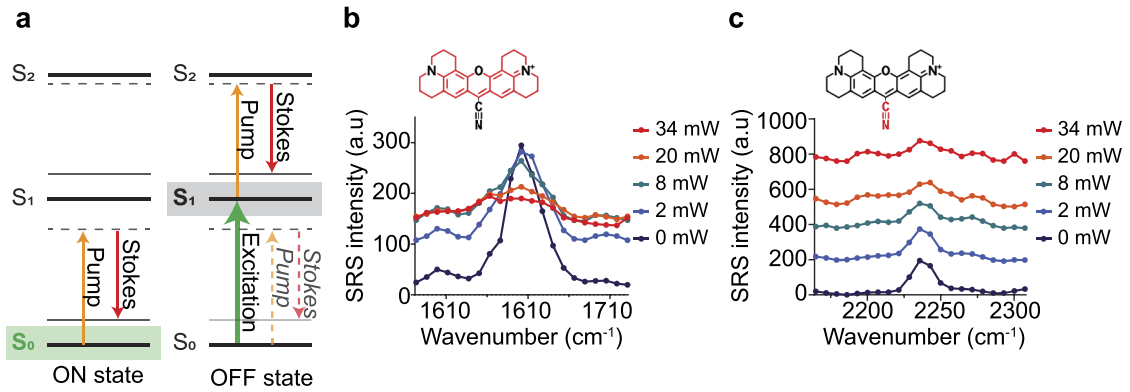

FIG. 2. Photoswitching of epr-SRS signals via transition to the electronic excited state. (a) Energy diagrams of the proposed ON (left, the green shade indicates the ground state as the ON state) and OFF (right, the gray shade indicates the excited state as the OFF state) states for epr-SRS signals. (b) epr-SRS spectra of the conjugated double bond mode (i.e., highlighted red in the molecular structure) of Rh800 at 0, 2, 8, 20, and 34 mW of 660 nm excitation beam irradiation. (c) epr-SRS spectra of the triple bond mode (red colored in the molecular structure) of Rh800 at 0, 2, 8, 20, and 34 mW of 660 nm excitation beam irradiation.

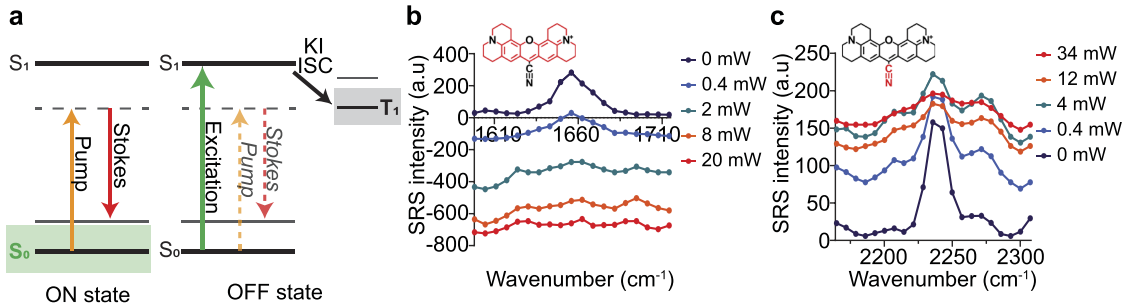

FIG. 3. Photoswitching of epr-SRS signals via transition to the triplet state. (a) Energy diagrams of the proposed ON (left, the green shade indicates the ground state as the ON state) and OFF (right, the gray shade indicates the triplet state as the OFF state) states for epr-SRS signals. (b) epr-SRS spectra of the double-bond mode (red-colored in the molecular structure) of Rh800 at 0, 0.4, 2, 8, and 20 mW of 660 nm excitation beam power in the presence of potassium iodide (KI). (c) epr-SRS spectra of the triple-bond mode (red colored in the molecular structure) of Rh800 at 0, 0.4, 4, 12, and 34 mW of 660 nm excitation beam power in the presence of (KI).

spin–orbit coupling.[32–34] The increase in triplet state population was confirmed by fluorescence intensity measurements (Fig. S3). Similar to the excited state SRS spectra, the double bond [Fig. 3(b) and Fig. S4(a)] and triple bond [Fig. 3(c) and Fig. S4(b)] peaks disappeared when the Rh800 molecules were further shifted to the triplet state in the presence of KI. Surprisingly, while we still detected a large background increase for the triple-bond peaks, we observed a large negative background signal across the double-bond frequency range.

These negative signals indicate an increase in pump photons, since we detected the stimulated Raman loss (i.e., the pump photon loss) as SRS signals (see the Methods section). Although a complete understanding of the molecular pathways would require further studies, a plausible reason for such an increase in pump photons is the population depletion in the presence of Stokes photons due to the excitation competition for the T_1–T_n transitions. Since the pump beam wavelength for the triple-bond excitation (i.e., 838 nm) is further blue shifted from that for the double bond (i.e., 880 nm) and from the Stokes beam (i.e., 1031.2 nm), it is possible that 838 nm light falls out of the T_1–T_n transition range, and hence do not induce a significant negative background. Here, we successfully demonstrated that both the excited state and the triplet state could effectively deprive the epr-SRS signals for both the double and the triple bond of the Rh800 molecules. However, both induced negative and positive electronic backgrounds, which could introduce artifacts in analyzing the epr-SRS images. In addition, inducing transitions to the excited and triplet state would lead to increased photobleaching. We hence continued to explore two other molecular states as the effective OFF state.

B. Photoswitching by modulating the epr-SRS enhancement: Organic dyes

The third electronic state we aimed at exploiting was the long-lived reversible dark state (~100 ms to s in an oxygenated environment). This photo-reduced state in the presence of electron donors for organic fluorophores has been heavily explored in STORM and d-STORM super-resolution fluorescence microscopy. For example, oxazine and rhodamine dyes are known to form semi-reduced radicals ($F^{\cdot}$) or leuco (FH) structures in buffers containing primary thiols (RSH) upon irradiations to the triplet state (^3F) [Fig. 4(a), gray box, RS-indicates the thiolate anions].[35] Similarly, cyanine dyes have also been shown to form a cyanine-thiol adduct under similar excitation and buffer conditions.[36] A photophysical change associated with this photochemical reduction is the diminishment of the electronic absorption peaks. Since epr-SRS signals strongly depend on the oscillation strength of the molecular absorption (see the supplementary material, Scheme 1, parameter K),[20,37] the disappearance of absorption peaks in these photo-reduced states indicates that they would be ideal candidates to serve as the OFF state for epr-SRS excitations [Fig. 4(a) OFF state, gray box].

We tested this hypothesis with ATTO680, a red-absorbing oxazine dye that falls into the desired electronic pre-resonance excitation region under our SRS laser excitation and was reported to undergo light-induced transitions to the above-mentioned long-lived dark state [Figs. 4(a) and 4(b)].[35] Exciting ATTO680 solutions containing primary thiol β-mercaptoethylamine (MEA) with a 660 nm excitation beam could indeed transform the color of the solutions into transparent [Fig. 4(c) vs Fig. 4(d), cuvette in the inset, before and after 660 nm illumination]. Subsequent absorption measurement confirmed the disappearance of the corresponding absorption peak for ATTO680 [Fig. 4(c) vs Fig. 4(d)]. The remnant absorption after irradiation [Fig. 4(d)] was due to a layer of unconverted molecules at the interface between the solution and the airspace of the cuvette. After gentle shaking of the cuvette to facilitate dissolution of oxygen in the headspace, both the color and the absorbance peaks of the same solution were fully recovered [Fig. 4(e)], which indicates that the molecules are relaxed back to the ground state ($^1F_0$). These results confirm that the absorption peaks of ATTO680 can be switched on and off, as reported.[38]

We next examined whether the same excitation and oxidation steps can switch the epr-SRS signals on and off. We followed the same excitation procedure but contained the sample solution in a glass chamber typically used for SRS measurement [Fig. 5(a)]. Indeed, we successfully observed reversibly switchable epr-SRS signals targeting the double bond peak of ATTO680 at 1661 cm^{-1} [Fig. 5(b), solid line, red]. The concurrent switching of the fluorescence over multiple cycles was also observed [Fig. 5(b), solid line, blue]. The reduced epr-SRS signals could reach as low as to 5% of the original epr-SRS intensity. Control experiments in the absence

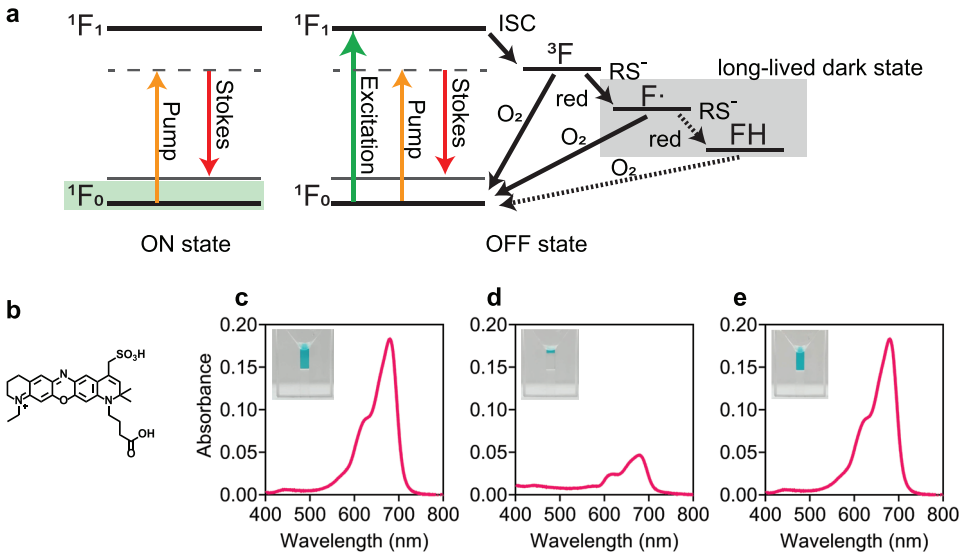

FIG. 4. Proposed strategy to photoswitch epr-SRS signals via transition to the absorption diminished long-lived dark state. (a) Energy diagrams of the proposed ON (left, the green shade indicates the ground state as the ON state) and OFF (right, the gray shade indicates the long-lived dark state as the OFF state) states. $^1F_0$, singlet ground state; $^1F_1$, singlet excited state; ^3F, triplet state; F$^{\cdot}$, semireduced radical state; FH, fully reduced leuco state; ISC, intersystem crossing; red, reduction; and RS$^-$, thiolate anions. (b) Molecular structure of ATTO680. [(c)–(e)] Absorption spectra of ATTO680 before (c) and after (d) irradiating with a 660 nm excitation beam, and after agitating the cuvette to facilitate oxidation (e). Insets show the images of solution color change in the same cuvette.

of MEA showed no effect of such photoswitching [Fig. 5(b), dotted line, red for epr-SRS and blue for fluorescence signals]. Together, these data confirm that shifting the molecules between the ground state and the photo-reduced dark state could serve as an effective strategy to photoswitch epr-SRS signals.

Although we have demonstrated the recovery of epr-SRS signals by mechanically accelerating the oxidation through shaking or pipetting the solutions, it is more appealing to utilize light to recover SRS signals for the precise control of the activation kinetics. As the oxidation of semi-reduced radicals is known to be accelerated by irradiation of UV light,[35] we asked whether we could turn the epr-SRS signals on from the dark state by illumination with a 405 nm laser instead. We observed that the 405 nm laser irradiation could increase the epr-SRS signals by 1.7 times compared to that from the OFF state [Fig. 5(c), green vs pink]. Fluorescence signals also showed a similar level of recovery (Fig. S5). We note that such a recovery was not observed in the absence of the 405 nm activation [Fig. 5(d)], implying that the recovery was not caused by other processes such as diffusion.

Going beyond the solution characterization, we further confirmed this photoswitching effect in epr-SRS imaging. 5-ethynyl-2′-deoxyuridine (EdU) was incorporated into newly synthesized DNA of dividing HeLa cells and was then click-labeled by ATTO680 azide. The labeled cells immersed in a MEA-containing buffer were subsequently imaged by epr-SRS, targeting the 1661 cm^{-1} peak of ATTO680 [Fig. 5(e)]. After sequential irradiation of the excitation beam and the 405 nm beam, the epr-SRS signals from ATTO680 (1661 cm^{-1}) were first decreased to 50% and then recovered back to 70% of the original signals [Figs. 5(e)–5(h)]. The limited depletion of the SRS signals in cell samples compared to solutions is likely due to the restricted transport of the thiolate anions in cells. We note that the limited recovery of the SRS signals after 405 nm irradiation [Figs. 5(c) and 5(h), green] should be due to the fact that ATTO680 has a high electron affinity and accepts another electron to form a leuco dye (FH) [Fig. 4(a)].[38] As this leuco dye is more stable than the semi-reduced radical (F$^{\cdot}$), the oxidation is not easily facilitated by the 405 nm laser. Screening other rhodamine and oxazine dyes with a stable dark-state in the semi-reduced radical form should further increase the activation efficiency. However, such currently known structures (e.g., ATTO532) mostly fall outside the desired epr-SRS excitation regime (640–790 nm). Shifting the wavelength of SRS lasers to the bluer region, as recently reported, should facilitate screening of better performing photoswitchable epr-SRS probes.[39,40]

C. Photoswitching by modulating the epr-SRS enhancement: Photoswitchable proteins

Based on the pre-resonance Raman approximation,[19,20,37] epr-SRS signals are nonlinearly dependent on another photophysical parameter, the detuning between the pump photon energy and the molecular electronic resonance [see supplementary material, Scheme 1, parameter $\frac{1}{(\omega_0^2-\omega_{pump}^2)^4}$]. The epr-SRS signals would decrease over 10^5-fold when the pump laser energy (ω_{pump}) is detuned away from the molecular electronic transition energy (ω_0).[20] Therefore, molecules with switchable electronic resonances closer to and further away from the pump laser energy could also serve as ON and OFF epr-SRS states, respectively, with a decent ON-to-OFF ratio [Fig. 6(a)].[41] We tested a recently engineered truncated version of a reversibly switchable far-red absorbing soluble bacterial phytochrome photoreceptor (BphP) from *Deinococcus radiodurans*, DrBphP-PCM [Fig. 6(b)].[42] The absorbing core of DrBphP-PCM is composed of a photosensory core module (PCM), which is shared by all BphPs, and a covalently attached biliverdin IXa chromophore, which is the enzymatic product of heme catabolism and present in all mammalian cells. Biliverdin undergoes reversible *cis–trans* isomerization when irradiated with different wavelengths of light, causing BphP transitions between two

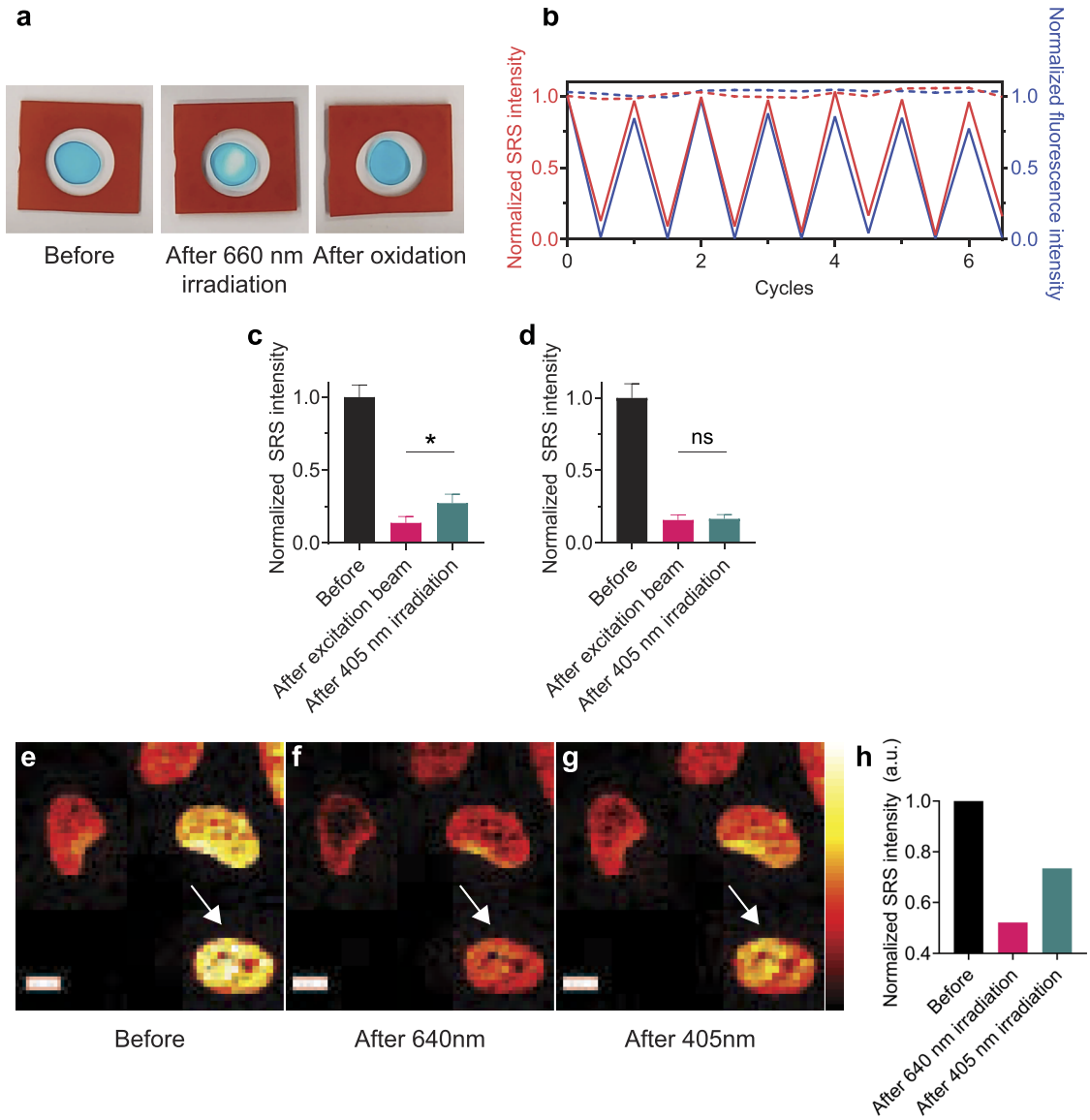

FIG. 5. Photoswitching of epr-SRS signals via transition to the long-lived dark state. (a) A photo of ATTO680 solution containing 0.5M MEA at pH 9.5 in an SRS imaging chamber before (left) and after (middle) excitation beam irradiation, and after oxidation (right). (b) Reversible switching of epr-SRS (red) and fluorescence (blue) signals for multiple cycles of irradiation and oxidation (solid line). No switching was observed in the absence of MEA for both epr-SRS (red) and fluorescence (blue) (dashed line). (c) epr-SRS signals before (black) and after (magenta) excitation beam, and after 405 nm activation (green) irradiation. (d) epr-SRS signals of ATTO680 solutions without 405 nm activation. [(e)–(g)] epr-SRS images of ATTO680-click-labeled DNA in HeLa cells before irradiation (e), after excitation beam irradiation (f), and after 405 nm laser irradiation (g). (h) Quantification of epr-SRS signals from the arrowed cell in (e)–(g). Scale bars, 10 μM. In (c) and (d), statistical significance was determined by the unpaired two tailed *t* test. ns, not significant ($p > 0.05$), *$p < 0.05$. Data are shown as mean ± standard deviation (n = 3 replicates for each group).

absorbing states, Pr and Pfr [Fig. 6(b), *cis–trans* isomerization highlighted in the blue circle].[42] With purified DrBphP-PCM solutions, we first confirmed their reversibly switchable absorptions, peaked at 750 nm [Fig. 6(c), magenta, the Pfr state in Fig. 6(b)] and 700 nm [Fig. 6(c), black, the Pr state in Fig. 6(b)], upon illumination with 690 and 780 nm, respectively.

We next quantified its epr-SRS signal magnitude and reversibility. As the absorption peaks of DrBphP-PCM fall within the desired epr-SRS excitation regime,[19,20] DrBphP-PCM in its epr-SRS ON state (i.e., the Pfr state) shows an around 300 times signal magnitude to that of EdU, adopting the recent RIE (the relative intensity to EdU) quantification metrics [Fig. 6(d)].[43] Such a signal size is

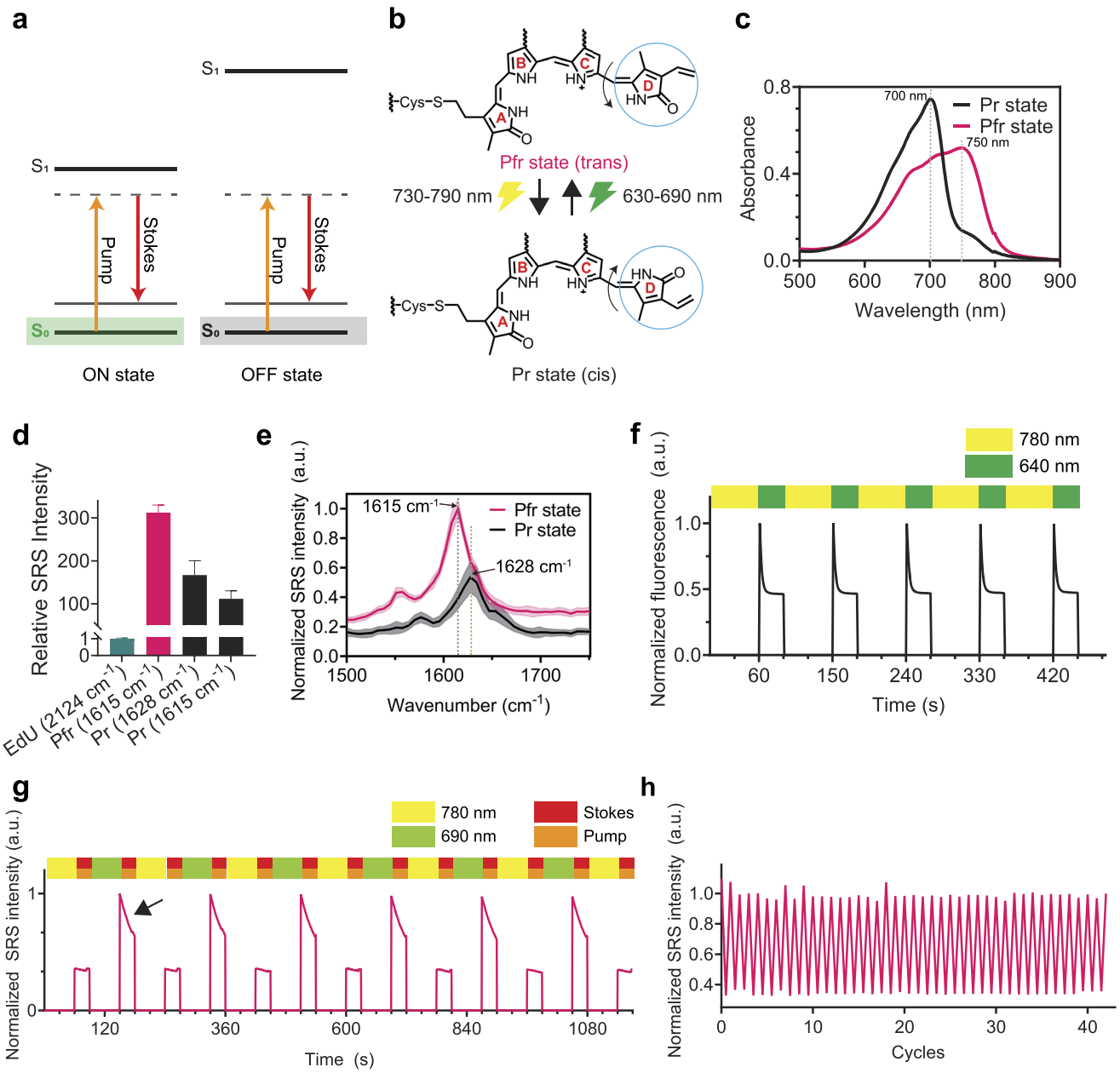

FIG. 6. Photoswitching of the purified near-infrared absorbing DrBphP-PCM protein. (a) Energy diagrams of the proposed ON (left, green shaded) and OFF (right, gray shaded) states. (b) *Cis–trans* configuration change of the biliverdin chromophore in DrBphP-PCM upon irradiation. (c) Absorption spectra of DrBphP-PCM in the Pr (black) and Pfr (magenta) conformation states. (d) Relative epr-SRS signals of DrBphP-PCM in the Pfr (1615 cm^{-1}, magenta) and Pr (both 1628 cm^{-1}, black; and 1615 cm^{-1}, brown) states compared to the standard SRS signal of EdU (2124 cm^{-1}, green). (e) epr-SRS spectra of DrBphP-PCM in the Pr (black) and Pfr (magenta) states. (f) Cycles of reversible photoswitching of DrBphP-PCM fluorescence, observed in the Pr state. (g) Cycles of reversible photoswitching of DrBphP-PCM epr-SRS signal at 1615 cm^{-1}, the ON state (Pfr state) on-resonance channel. (h) Photoswitching of DrBphP-PCM at 1615 cm^{-1} for over 40 cycles demonstrates no detectable photofatigue.

equivalent to a detection sensitivity below 1 μM for this probe.[44] When switched to the epr-SRS OFF state (i.e., the Pr state) by 780 nm laser, DrBphP-PCM indeed presents a lowered epr-SRS signal for the double bond mode with a Raman peak shifted from 1615 to 1628 cm^{-1} [Fig. 6(e), magenta and black, respectively]. This peak shift is resulted from the change in *cis–trans* conformation of the double bond between ring C and ring D of the biliverdin chromophore [Fig. 6(b)].[45] Detecting the absolute intensity changes at

the 1615 cm^{-1} channel yielded an about three-fold signal decrease between the epr-SRS ON and OFF states [Figs. 6(d) and 6(e)]. The residual 33% of epr-SRS signals in the OFF state [Figs. 6(d) and 6(e)] originates from a combination of the remaining epr-SRS enhancement from the OFF-state Raman peak and a slight electronic background by the pump laser from the relatively broad absorption bands of DrBphP-PCM [Fig. 6(c)].

After the initial characterization of DrBphP-PCM, we tested the robustness of the photo-switching for epr-SRS signals as the resistance to switching fatigue is an important photophysical parameter in reversibly switchable probes. We first monitored the cycles of reversibility for the DrBphP-PCM fluorescence signals using the sequence of alternating 60 and 30 s illuminations by the 780 nm [Fig. 6(f), yellow] and 640 nm [Fig. 6(f), green] lasers. The 780 nm laser switches the protein to the Pr state exhibiting a weak fluorescence peak at 720 nm,[46] whereas the 640 nm laser serves as both the readout laser and the deactivation laser that shifts the protein back to the Pfr non-fluorescent state. We note that the ON and OFF states for fluorescence signals are reversed from those of epr-SRS signals as quantum yields of the Pr and Pfr states are 2.9% and 0%, respectively.[46] Our observed fluorescence depletion and recovery are similar to what were reported previously [Fig. 6(f)].[42,46]

We then probed the reversibility of the epr-SRS signals. Here, a 780 nm laser was adopted as the deactivation laser, a 690 nm laser was used as the activation laser, and the SRS beams were used as the signal readout laser. Figure 6(g) shows the laser sequence and the corresponding epr-SRS ON and OFF intensity. Similar to that for fluorescence, clear photo-switching of epr-SRS signals was observed over multiple cycles [Fig. 6(g)], whereas the epr-SRS signal levels remained unchanged in the absence of the 690 nm and 780 nm lasers [Fig. S6(a)]. In a separate control experiment, we irradiated the protein solution with Stokes and pump beams for 30 s and allowed the molecules to diffuse and replenish for 60 s [Fig S6(b)]. However, no SRS recovery was observed [Fig. S6(b), dotted line]. In contrast, when the protein sample was irradiated by a 690 nm activation laser, the SRS signal immediately increased back to the original intensity [Fig. S6(b), green arrow]. This result indicates that the role of diffusion is minimal and shows that the recovery of SRS signals is not caused by diffusion of the ON molecules into the focal volume, but from activation via the 690 nm light.

Interestingly, we observed a decrease in the epr-SRS signals when the DrBphP-PCM solution was irradiated with SRS beams [Fig. 6(g), black arrow]. We attribute this switching-off effect to pump beam excitation (around 884 nm), which could excite at the very tail of the absorption peak of the Pfr state [Fig. 6(c), magenta]. We note that this decrease is not due to photobleaching, as epr-SRS signals always recovered back to 100% with 690 nm beam activation [Fig. 6(g)]. We further extended the epr-SRS switchable cycles to more than 40 cycles with minimum photobleaching, demonstrating the robustness of the DrBphP-PCM protein as a photoswitchable epr-SRS probe [Fig. 6(h)]. We reasoned that the minimal photobleaching observed here should likely be due to two reasons. First, the competing switching-off pathway from the SRS beams may have likely helped in reducing the potential photobleaching kinetics from either the one-photon or the two-photon excitation by the SRS lasers. Second, the adopted picosecond SRS beams should contribute much less to the higher-order multi-photon excitation induced photobleaching, since their peak power is much smaller compared to that of the femtosecond lasers.

III. DISCUSSION

This work presents a series of photophysical characterizations and proof-of-principle observations toward a new type of optical imaging probes, i.e., the photoswitchable epr-Raman probes. We explored the possibilities of four electronic states to serve as the effective OFF state for the epr-SRS signals. In our first two strategies, we induced transitions to the excited state and the triplet states, which led to successful reduction of the epr-SRS peaks. However, robust frequency-modulation SRS techniques are required to remove the large electronic background (both the positive and negative ones) for further applications.[30,31] Guided by the Albrecht A-term pre-resonance approximation equation (see the supplementary material, Scheme 1), we subsequently explored another two states, the long-lived dark state with a diminished absorption peak from organic dyes and a tunable absorption transition state with modulable detuning to the pump photon energy from photoswitchable proteins. We proved that all four states together with the ground state could serve as the ideal candidates for reversibly photo-switching the epr-SRS signals upon further optimizations through additional engineering and designing of the photoswitchable Raman probes.

As we indicated above, for red-absorbing organic molecules, extensive screening of rhodamine and oxazine dyes with a stable dark-state in the semi-reduced radical form should help improve the activation efficiency with 405 nm laser. In addition, cyanine dyes with a similar cyanine-thiol adduct may also offer new opportunities. In parallel with the dye screening, doubling the frequencies of the SRS lasers as recently demonstrated would offer the matching excitation region for molecules across the entire visible absorption range, vastly expanding the pools for photo-switchable epr-SRS probes.[39,40]

We have also demonstrated that the DrBphP-PCM protein shows high promise toward generating a new category of photoswitchable Raman proteins. Further protein engineering efforts for obtaining larger dynamic ranges of the ON-to-OFF signal ratios are required. This would offer multiplexable epr-SRS peaks and allow genetical encodability for future cell imaging applications. First, slightly blue shifting the absorption peak (e.g., for 30–50 nm) would minimize the electronic background. This would lead to a clearer separation of Raman peaks between the epr-SRS ON and OFF states for easier multiplexing. Second, larger shift in absorption peaks between the epr-SRS ON and OFF states should also contribute to enhancing the dynamic ranges of the ON-to-OFF ratios. Third, mutagenesis of the amino acid residues around the biliverdin binding pocket may shift its double bond vibrational frequency by changing the interacting environment and, hence, creating more colors.[47] Fourth, incorporation of a nitrile bond to the conjugation system of the biliverdin would significantly help expand the epr-SRS color palette owing to the features of the narrow-band and editable nitrile bonds that are ideal for multiplexing. Fifth, the superior property of photoswitchable Raman protein-based probes is their genetic encodability, which is critical for live cell imaging

and is not offered by organic dyes. Moreover, it is worth noting that whereas photoswitching of organic dyes frequently requires UV light, which is phototoxic for cells, the Raman protein probes derived from BphPs use non-cytotoxic photoswitching far-red and near-infrared light, which penetrates much deeper in biological tissues, thus enabling intravital imaging.[48] Further engineering of distinct BphP-based Raman probes, along with their different intracellular targeting, will allow super-multiplex epr-SRS imaging in live cells.

Ultimately, with successful invention of a new category of photoswitchable epr-SRS probes, super-multiplex super-resolution optical imaging may be implemented, as we rationalized above. Adopting a doughnut setup similar to RESOLFT but with only one additional switching laser, super-multiplex imaging could be brought into the super-resolution regime and offer a valuable new addition to the toolbox of optical imaging in investigating biological activities and functions.

SUPPLEMENTARY MATERIAL

See the supplementary material for experimental methods, scheme, supporting figures, and tables.

ACKNOWLEDGMENTS

This work was supported by the grants from the National Institutes of Health, Grant No. DP2 GM140919 (to L.W.) and Grant No. R35 GM122567 (to V.V.), and by the start-up fund from the California Institute of Technology (to L.W.).

DATA AVAILABILITY

The data that support the findings of this study are available from the corresponding author upon reasonable request.

REFERENCES

[1] R. Ando, H. Mizuno, and A. Miyawaki, "Regulated fast nucleocytoplasmic shuttling observed by reversible protein highlighting," Science **306**(5700), 1370–1373 (2004).
[2] G. U. Nienhaus, K. Nienhaus, A. Hölzle, S. Ivanchenko, F. Renzi, F. Oswald, M. Wolff, F. Schmitt, C. Röcker, B. Vallone, W. Weidemann, R. Heilker, H. Nar, and J. Wiedenmann, "Photoconvertible fluorescent protein EosFP: Biophysical properties and cell biology applications," Photochem. Photobiol. **82**(2), 351–358 (2006).
[3] J. Lippincott-Schwartz and G. H. Patterson, "Photoactivatable fluorescent proteins for diffraction-limited and super-resolution imaging," Trends Cell Biol. **19**(11), 555–565 (2009).
[4] Y.-T. Kao, X. Zhu, and W. Min, "Protein-flexibility mediated coupling between photoswitching kinetics and surrounding viscosity of a photochromic fluorescent protein," Proc. Natl. Acad. Sci. U. S. A. **109**(9), 3220–3225 (2012).
[5] X. X. Zhou and M. Z. Lin, "Photoswitchable fluorescent proteins: Ten years of colorful chemistry and exciting applications," Curr. Opin. Chem. Biol. **17**(4), 682–690 (2013).
[6] T. A. Klar and S. W. Hell, "Subdiffraction resolution in far-field fluorescence microscopy," Opt. Lett. **24**(14), 954–956 (1999).
[7] E. Betzig, G. H. Patterson, R. Sougrat, O. W. Lindwasser, S. Olenych, J. S. Bonifacino, M. W. Davidson, J. Lippincott-Schwartz, and H. F. Hess, "Imaging intracellular fluorescent proteins at nanometer resolution," Science **313**(5793), 1642–1645 (2006).
[8] M. J. Rust, M. Bates, and X. Zhuang, "Sub-diffraction-limit imaging by stochastic optical reconstruction microscopy (STORM)," Nat. Methods **3**(10), 793–796 (2006).
[9] M. Hofmann, C. Eggeling, S. Jakobs, and S. W. Hell, "Breaking the diffraction barrier in fluorescence microscopy at low light intensities by using reversibly photoswitchable proteins," Proc. Natl. Acad. Sci. U. S. A. **102**(49), 17565–17569 (2005).
[10] M. Andresen, A. C. Stiel, J. Fölling, D. Wenzel, A. Schönle, A. Egner, C. Eggeling, S. W. Hell, and S. Jakobs, "Photoswitchable fluorescent proteins enable monochromatic multilabel imaging and dual color fluorescence nanoscopy," Nat. Biotechnol. **26**(9), 1035–1040 (2008).
[11] S. J. Sahl, S. W. Hell, and S. Jakobs, "Fluorescence nanoscopy in cell biology," Nat. Rev. Mol. Cell Biol. **18**(11), 685–701 (2017).
[12] F. Lavoie-Cardinal, N. A. Jensen, V. Westphal, A. C. Stiel, A. Chmyrov, J. Bierwagen, I. Testa, S. Jakobs, and S. W. Hell, "Two-color RESOLFT nanoscopy with green and red fluorescent photochromic proteins," ChemPhysChem **15**(4), 655–663 (2014).
[13] I. Testa, E. D'Este, N. T. Urban, F. Balzarotti, and S. W. Hell, "Dual channel RESOLFT nanoscopy by using fluorescent state kinetics," Nano Lett. **15**(1), 103–106 (2015).
[14] C. W. Freudiger, W. Min, B. G. Saar, S. Lu, G. R. Holtom, C. He, J. C. Tsai, J. X. Kang, and X. S. Xie, "Label-free biomedical imaging with high sensitivity by stimulated Raman scattering microscopy," Science **322**(5909), 1857–1861 (2008).
[15] B. G. Saar, C. W. Freudiger, J. Reichman, C. M. Stanley, G. R. Holtom, and X. S. Xie, "Video-rate molecular imaging in vivo with stimulated Raman scattering," Science **330**(6009), 1368–1370 (2010).
[16] J.-X. Cheng and X. S. Xie, "Vibrational spectroscopic imaging of living systems: An emerging platform for biology and medicine," Science **350**(6264), aaa8870 (2015).
[17] L. Wei, F. Hu, Z. Chen, Y. Shen, L. Zhang, and W. Min, "Live-cell bioorthogonal chemical imaging: Stimulated Raman scattering microscopy of vibrational probes," Acc. Chem. Res. **49**(8), 1494–1502 (2016).
[18] F. Hu, L. Shi, and W. Min, "Biological imaging of chemical bonds by stimulated Raman scattering microscopy," Nat. Methods **16**(9), 830–842 (2019).
[19] L. Wei, Z. Chen, L. Shi, R. Long, A. V. Anzalone, L. Zhang, F. Hu, R. Yuste, V. W. Cornish, and W. Min, "Super-multiplex vibrational imaging," Nature **544**(7651), 465–470 (2017).
[20] L. Wei and W. Min, "Electronic preresonance stimulated Raman scattering microscopy," J. Phys. Chem. Lett. **9**(15), 4294–4301 (2018).
[21] H. Xiong, L. Shi, L. Wei, Y. Shen, R. Long, Z. Zhao, and W. Min, "Stimulated Raman excited fluorescence spectroscopy and imaging," Nat. Photonics **13**(6), 412–417 (2019).
[22] L. Möckl and W. E. Moerner, "Super-resolution microscopy with single molecules in biology and beyond–essentials, current trends, and future challenges," J. Am. Chem. Soc. **142**(42), 17828–17844 (2020).
[23] L. Schermelleh, A. Ferrand, T. Huser, C. Eggeling, M. Sauer, O. Biehlmaier, and G. P. C. Drummen, "Super-resolution microscopy demystified," Nat. Cell Biol. **21**(1), 72–84 (2019).
[24] M. Bates, G. T. Dempsey, K. H. Chen, and X. Zhuang, "Multicolor super-resolution fluorescence imaging via multi-parameter fluorophore detection," ChemPhysChem **13**(1), 99–107 (2012).
[25] J. Bückers, D. Wildanger, G. Vicidomini, L. Kastrup, and S. W. Hell, "Simultaneous multi-lifetime multi-color STED imaging for colocalization analyses," Opt. Express **19**(4), 3130–3143 (2011).
[26] R. Wilbrandt, N. H. Jensen, P. Pagsberg, A. H. Sillesen, and K. B. Hansen, "Triplet state resonance Raman spectroscopy," Nature **276**(5684), 167–168 (1978).
[27] S. Rieger, M. Fischedick, K.-J. Boller, and C. Fallnich, "Suppression of resonance Raman scattering via ground state depletion towards sub-diffraction-limited label-free microscopy," Opt. Express **24**(18), 20745 (2016).
[28] P. Kukura, D. W. McCamant, and R. A. Mathies, "Femtosecond stimulated Raman spectroscopy," Annu. Rev. Phys. Chem. **58**(1), 461–488 (2007).

[29]L. Shi, H. Xiong, Y. Shen, R. Long, L. Wei, and W. Min, "Electronic resonant stimulated Raman scattering micro-spectroscopy," J. Phys. Chem. B **122**(39), 9218–9224 (2018).
[30]D. Zhang, M. N. Slipchenko, D. E. Leaird, A. M. Weiner, and J.-X. Cheng, "Spectrally modulated stimulated Raman scattering imaging with an angle-to-wavelength pulse shaper," Opt. Express **21**(11), 13864–13874 (2013).
[31]D. Fu, W. Yang, and X. S. Xie, "Label-free imaging of neurotransmitter acetylcholine at neuromuscular junctions with stimulated Raman scattering," J. Am. Chem. Soc. **139**(2), 583–586 (2017).
[32]A. Chmyrov, T. Sandén, and J. Widengren, "Iodide as a fluorescence quencher and promoter—Mechanisms and possible implications," J. Phys. Chem. B **114**(34), 11282–11291 (2010).
[33]E. Gatzogiannis, X. Zhu, Y.-T. Kao, and W. Min, "Observation of frequency-domain fluorescence anomalous phase advance due to dark-state hysteresis," J. Phys. Chem. Lett. **2**(5), 461–466 (2011).
[34]J. Widengren, U. Mets, and R. Rigler, "Fluorescence correlation spectroscopy of triplet states in solution: A theoretical and experimental study," J. Phys. Chem. **99**(36), 13368–13379 (1995).
[35]S. van de Linde, A. Löschberger, T. Klein, M. Heidbreder, S. Wolter, M. Heilemann, and M. Sauer, "Direct stochastic optical reconstruction microscopy with standard fluorescent probes," Nat. Protoc. **6**(7), 991–1009 (2011).
[36]G. T. Dempsey, M. Bates, W. E. Kowtoniuk, D. R. Liu, R. Y. Tsien, and X. Zhuang, "Photoswitching mechanism of cyanine dyes," J. Am. Chem. Soc. **131**(51), 18192–18193 (2009).
[37]A. C. Albrecht and M. C. Hutley, "On the dependence of vibrational Raman intensity on the wavelength of incident light," J. Chem. Phys. **55**(9), 4438–4443 (1971).
[38]S. van de Linde, I. Krstić, T. Prisner, S. Doose, M. Heilemann, and M. Sauer, "Photoinduced formation of reversible dye radicals and their impact on super-resolution imaging," Photochem. Photobiol. Sci. **10**(4), 499–506 (2011).
[39]H. Xiong, N. Qian, Y. Miao, Z. Zhao, and W. Min, "Stimulated Raman excited fluorescence spectroscopy of visible dyes," J. Phys. Chem. Lett. **10**(13), 3563–3570 (2019).
[40]Y. Bi, C. Yang, Y. Chen, S. Yan, G. Yang, Y. Wu, G. Zhang, and P. Wang, "Near-resonance enhanced label-free stimulated Raman scattering microscopy with spatial resolution near 130 nm," Light: Sci. Appl. **7**, 81 (2018).
[41]H. Fujioka, J. Shou, R. Kojima, Y. Urano, Y. Ozeki, and M. Kamiya, "Multicolor activatable Raman probes for simultaneous detection of plural enzyme activities," J. Am. Chem. Soc. **142**, 20701 (2020).
[42]L. Li, A. A. Shemetov, M. Baloban, P. Hu, L. Zhu, D. M. Shcherbakova, R. Zhang, J. Shi, J. Yao, L. V. Wang, and V. V. Verkhusha, "Small near-infrared photochromic protein for photoacoustic multi-contrast imaging and detection of protein interactions in vivo," Nat. Commun. **9**(1), 2734 (2018).
[43]H. Yamakoshi, K. Dodo, A. Palonpon, J. Ando, K. Fujita, S. Kawata, and M. Sodeoka, "Alkyne-tag Raman imaging for visualization of mobile small molecules in live cells," J. Am. Chem. Soc. **134**(51), 20681–20689 (2012).
[44]L. Wei, F. Hu, Y. Shen, Z. Chen, Y. Yu, C.-C. Lin, M. C. Wang, and W. Min, "Live-cell imaging of alkyne-tagged small biomolecules by stimulated Raman scattering," Nat. Methods **11**(4), 410–412 (2014).
[45]C. Kneip, P. Hildebrandt, W. Schlamann, S. E. Braslavsky, F. Mark, and K. Schaffner, "Protonation state and structural changes of the tetrapyrrole chromophore during the $P_r \rightarrow P_{fr}$ phototransformation of phytochrome: A resonance Raman spectroscopic study," Biochemistry **38**(46), 15185–15192 (1999).
[46]V. V. Lychagov, A. A. Shemetov, R. Jimenez, and V. V. Verkhusha, "Microfluidic system for in-flow reversible photoswitching of near-infrared fluorescent proteins," Anal. Chem. **88**(23), 11821–11829 (2016).
[47]S. D. Fried, S. Bagchi, and S. G. Boxer, "Extreme electric fields power catalysis in the active site of ketosteroid isomerase," Science **346**(6216), 1510–1514 (2014).
[48]D. M. Shcherbakova, O. V. Stepanenko, K. K. Turoverov, and V. V. Verkhusha, "Near-infrared fluorescent proteins: Multiplexing and optogenetics across scales," Trends Biotechnol. **36**(12), 1230–1243 (2018).